Vol 17 No 3, March 2008
1674-1056/2008/17(03)/1119-05
Chinese Physics B
© 2008 Chin. Phys. Soc.
and IOP Publishing Ltd

Influence of V/III ratio on the structural and photoluminescence properties of $In_{0.52}AlAs/ In_{0.53}GaAs$ metamorphic high electron mobility transistor grown by molecular beam epitaxy

Gao Hong-Ling(高宏玲)[a)†], Zeng Yi-Ping(曾一平)[a)], Wang Bao-Qiang(王宝强)[a)], Zhu Zhan-Ping(朱战平)[a)], and Wang Zhan-Guo(王占国)[b)]

[a)] *Novel Materials Laboratory, Institute of Semiconductors, Chinese Academy of Sciences, Beijing* 100083, *China*

[b)] *Key Laboratory of Semiconductor Materials Science, Institute of Semiconductors, Chinese Academy of Sciences, Beijing* 100083, *China*

(Received 8 August 2007; revised manuscript received 8 October 2007)

A series of metamorphic high electron mobility transistors (MMHEMTs) with different V/III flux ratios are grown on GaAs (001) substrates by molecular beam epitaxy (MBE). The samples are analysed by using atomic force microscopy (AFM), Hall measurement, and low temperature photoluminescence (PL). The optimum V/III ratio in a range from 15 to 60 for the growth of MMHEMTs is found to be around 40. At this ratio, the root mean square (RMS) roughness of the material is only 2.02 nm; a room-temperature mobility and a sheet electron density are obtained to be 10610.0$cm^2/(V\cdot s)$ and $3.26\times10^{12}cm^{-2}$ respectively. These results are equivalent to those obtained for the same structure grown on InP substrate. There are two peaks in the PL spectrum of the structure, corresponding to two sub-energy levels of the $In_{0.53}Ga_{0.47}As$ quantum well. It is found that the photoluminescence intensities of the two peaks vary with the V/III ratio, for which the reasons are discussed.

Keywords: molecular beam epitaxy, semiconducting III–V materials, high electron mobility transistors

PACC: 7360L, 6855, 7855

1. Introduction

In the field of high electron mobility transistors (HEMTs), $In_{0.52}Al_{0.48}As/ In_{0.53}Ga_{0.47}As$ HEMTs on InP substrates are attractive devices for high-speed, low-voltage power amplifier applications.[1,2] However, InP substrates are more expensive, fragile, available only in smaller sizes, and processing technology less mature than that for GaAs. Therefore, InAlAs/InGaAs devices employing GaAs as substrates, called metamorphic HEMTs (MMHEMTs), have emerged. $In_{0.52}Al_{0.48}As/In_xGa_{1-x}As$ MMHEMT devices for high-speed digital and microwave applications have aroused much interest both in their potential device applications and in their fundamental physics. The study on MMHEMTs has focused on finding higher conduction-band discontinuities between InAlAs barrier and InGaAs well layers and a narrower band gap in the InGaAs channel to improve both the sheet carrier density n_s and mobility μ.[3–6] However, as an important factor during molecular beam epitaxy (MBE), the effects of the V/III ratio on the photoluminescence and structural properties of MMHEMTs are still unaddressed in the literature. In the present study, a series of $In_{0.52}Al_{0.48}As/ In_{0.53}Ga_{0.47}As$ MMHEMTs are grown under various V/III flux ratios on GaAs (001) substrates by MBE. Hall measurement, AFM, and low temperature PL are used to characterize the material, electrical, and optical properties of the MMHEMTs.

2. Experimental procedure

The schematic of a single δ-doping InGaAs/InAlAs MMHEMT structure is shown in Fig.1. The samples were grown by MBE on n-type GaAs(100) substrates by using an EPI GEN-II MBE system. Prior to the growth, surface oxide desorption was carried out under As_4 flux of 6.7×10^{-3}Pa beam equivalent pressure. The surface oxide was desorbed by slowly ramping up the substrate temperature

†E-mail: hlgao@semi.ac.cn

until the reflection high energy electron diffraction (RHEED) pattern showed an abrupt transformation to a 2×4 surface reconstruction. This surface reconstruction was adopted as a means for calibrating the substrate temperature, which was measured by using an infrared pyrometer with a suitable wavelength sensitivity. To ensure a smooth surface for epitaxial growth, an undoped GaAs buffer layer of about 80nm in thickness was first grown at a substrate temperature of 580°C. Then the substrate temperature was lowered to 340°C to grow the step-graded $In_yAl_{1-y}As$ buffer layers. The indium compositional gradient of the five step-graded InAlAs buffer layers was about 10% and each step of $In_yAl_{1-y}As$ is 100nm thick. At this growth temperature, 2D growth could be maintained. Then a 100nm thick $In_{0.52}Al_{0.48}As$ layer was grown at 480°C, followed by a 14nm thick $In_{0.53}Ga_{0.47}As$ channel layer, a 10nm thick $In_{0.52}Al_{0.48}As$ spacer layer, a Si δ-doping of $4\times10^{12}cm^{-2}$, a 36nm thick undoped $In_{0.52}Al_{0.48}As$ layer, and a 20 nm thick undoped $In_{0.53}Ga_{0.47}As$ cap layer. The growth rates of $In_{0.53}Ga_{0.47}As$ and $In_{0.52}Al_{0.48}As$ both were about 0.9μm/h. The V/III ratios varied from 15 to 60.

$In_{0.53}Ga_{0.47}As$ cap layer	20nm
$In_{0.52}Al_{0.48}As$	36nm
Si δ-doping	
$In_{0.52}Al_{0.48}As$ spacer	10nm
$In_{0.53}Ga_{0.47}As$ channel	14nm
$In_{0.52}Al_{0.48}As$	100nm
$In_{0.52}Al_{0.48}As$	100nm
$In_{0.40}Al_{0.60}As$	100nm
$In_{0.30}Al_{0.70}As$	100nm
$In_{0.20}Al_{0.80}As$	100nm
$In_{0.10}Al_{0.90}As$	100nm
GaAs buffer	80nm
Semi-insulating GaAs substrate	

Fig.1. Schematic cross section of the InGaAs/InAlAs metamorphic HEMT studied in this work.

We determined the V/III ratio from the following equation to be[7]

$$J_V/J_{III} = (P_V I_{III}/P_{III} I_V)\sqrt{(T_V M_{III}/T_{III} M_V)},$$

where P_V and P_{III} are the ionization gauge readings; I_V and I_{III} are the ionization cross-sections; M_V and M_{III} are the molecular weights of the beam species; and T_V and T_{III} are the temperatures of the species in the molecular beams (in Kelvin), which are taken to be the same as the source temperatures.

The MMHEMT samples with different V/III ratios were characterized by several techniques. Room temperature Hall measurement was carried out to obtain 2DEG density and mobility by using the van der Pauw–Hall method. The surface morphology of the samples was characterized by contact mode AFM. The PL measurements were obtained with a Fourier transform spectrometer and Ge detector. The samples were cooled down to 77K by liquid N_2 and excited with the 514.5nm line of an Ar^+ laser in a low-intensity limit (a few tens mW/cm^2).

3. Results and discussion

3.1. Hall measurements

Table 1 gives the Hall measurement results of the samples with different V/III ratios. It can be seen that the electron concentration is very large but the mobility is only 39.0cm^2/(V·s) in sample A (with a V/III ratio of 15). The reason may be that the excessively low V/III ratio may cause the decrease of the surface migration length of As_4 molecules and so lead to the local metallization of group III in the epitaxial layers.[8] With the V/III ratio increasing from 30 to 40, the electron concentration increases from $2.81\times10^{12}cm^{-2}$ to around $3.26\times10^{12}cm^{-2}$ while the electron mobility first increases and then decreases. This indicates that increasing the V/III ratio from 30 to 40 can improve the crystal quality of the material, and so increase the electron concentration and the electron mobility. Sample C was grown at a V/III ratio of 40, and it has a room-temperature mobility of 10610.0cm^2/(V·s) and a sheet electron density of $3.26\times10^{12}cm^{-2}$. These results are equivalent to those obtained from the sample with the same structure grown on an InP substrate. However, with V/III ratio further increasing from 40 to 60, the disorder degree in the material increases, i.e. more random distributions of Al, Ga and In on the group III sublattice have formed.[9] Thus the electron mobility of the 2DEG in the channel layer is reduced by the effect of the increase in the disorder degree of the material.

Table 1. Room temperature Hall measurement results of the samples with different V/III ratios.

sample	V/III ratio	electron concentration /($\times 10^{12}$cm^{-2})	electron mobility μ/(cm^2/(V·s))
A	15	3.46×10^3	39.0
B	30	2.81	8709.0
C	40	3.26	10610.0
D	50	3.24	8804.0
E	60	3.35	8482.0

On the other hand, at room temperature, remote ionized impurity scattering is not a dominant scattering mechanism. The polar optical phonon scattering, acoustic phonon scattering, alloy disorder scattering, and interface roughness scattering become the main scattering mechanisms that influence the electron mobility of the 2DEG.[10,11] The latter two are major factors related to the growth process. Comprehensively looking at the later AFM surface roughness measurements in Fig.2, we can find that at the beginning as the V/III ratio increases from 30 to 40, the crystal quality is improved, so the alloy disorder scattering and the interface roughness scattering decrease and the electron mobility increases. As the V/III ratio further increases from 40 to 60, the crystal quality and the roughness turn worse, causing its influence on the alloy disorder scattering and the interface roughness scattering to increase, and thus the electron mobility decreases.

3.2. AFM surface measurements

The morphological properties of the surface for samples A, B, C and D were investigated by AFM. Figure 2 shows the surface morphology recorded on a 5μm×5μm area for the MMHEMTs with different V/III flux ratios. A typical cross-hatch pattern is generated by the semi periodic roughness in the [110] and [1-10] in-plane directions except in sample A. The cross-hatch is triggered by the continual introduction of strain and consequent relaxation by the nucleation of 60° misfit dislocations from the graded $In_xAl_{1-x}As$ buffer layer.[12] The strain relaxation occurs due to the formation of 60° misfit dislocations parallel to the [1-10] (α dislocations) and [110] directions (β dislocations).

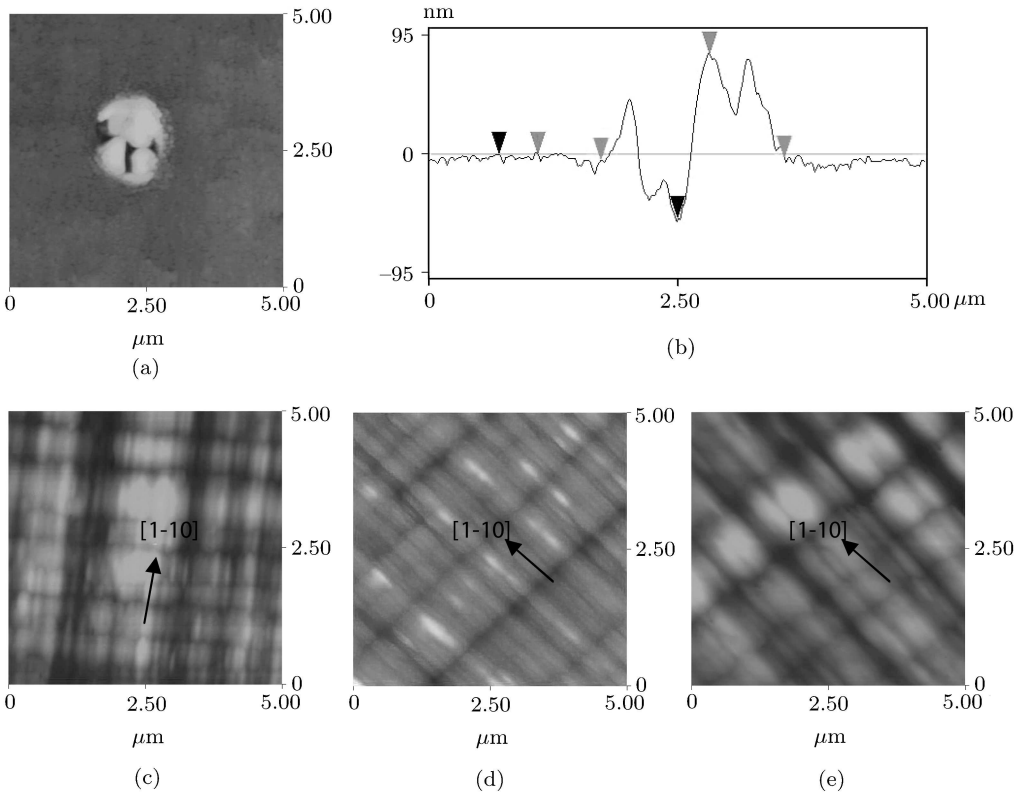


Fig.2. AFM surface morphologies of samples A(a), B(c), C(d), D(e) and section scans of the surface structure of sample A (b).

From Fig 2(a), we observe an island structure on the surface of sample A rather than the typical cross-hatch pattern. Using the sectional analysis mode of the AFM micrograph, one can determine the surface profiles near the island region (Fig.2(b)). The height and depth of the island are respectively about 80nm and 50nm with a lateral dimension of about 2μm. The SEM–EDS (scanning electron microscope–energy dispersive x-ray spectrometry) analysis indicates that the components of the island defects are nearly the same as those in the other regions, so the island defects are not caused by element deposition. This different surface morphology suggests that under a V/III ratio of 15 in sample A, the crystal quality is bad and the misfit stress during the buffer layer growth relaxes through the island defects rather than the cross-hatch structure.

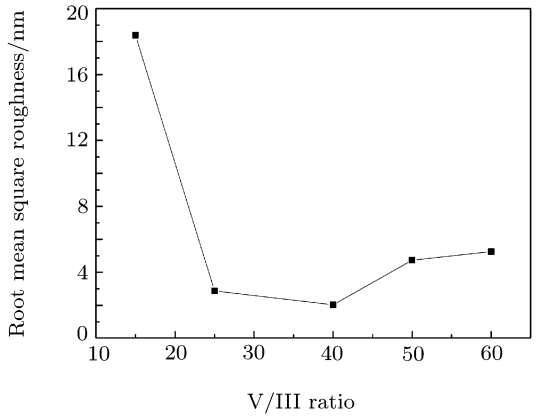


Fig.3. The surface RMS of the samples with different V/III ratios.

From Fig.3, when the V/III ratio increases to 30 in sample B, the surface turns smoothed and reaches an RMS roughness of 2.89nm. Sample C, grown at a V/III ratio of 40, has the smoothest surface morphology with a root mean square (RMS) roughness of 2.02 nm. This indicates that the increasing of the V/III ratio can modify the surface morphology. This modification of the surface reveals a correlation by which changing the V/III ratio can change the percentage of surface covered by As atoms that directly affect the surface structures of material in the MBE growth process.[13] At an appropriate As pressure, (2×4) surface structures will occur, of which the β (2×4) surface structure is most stable.[14] From Figs.2(c) and 2(d), we can see that sample C has the highest surface roughness, which indicates that in our experimental conditions, when the V/III ratio is around 40, the surface structures are β (2×4) surface structures. However, from Fig.3, with arsenic pressure further increasing, the surface roughnesses of the samples become worse in samples D and E because the increasing of the V/III ratio destroys the surface structure.

3.3. PL measurements

PL spectroscopy is a powerful tool for investigating the quality of a heterostructure. The 77K PL spectra of the samples are shown in Fig.4. Two transition peaks can be observed for samples in a photon energy range of 0.6–1.1eV. The higher energy peak in the PL spectra belongs to the transition from the second electron subband to the first heavy-hole subband (e_2-hh_1), and the lower energy peak belongs to the transition from the first electron subband to the first heavy-hole subband (e_2-hh_1) in the $In_{0.53}Ga_{0.47}As$ quantum well.[15]

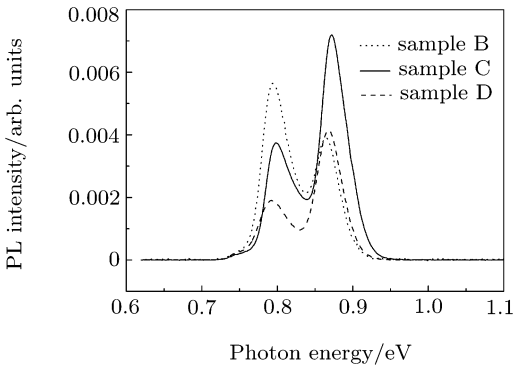


Fig.4. 77K PL spectra of the samples with different V/III ratios.

The results and calculations of many devices have shown that the peak intensity is governed by the wave function overlap between the two electron wave functions in the quantum well and that the ratio between intensities of the two transitions in the PL spectra can reflect the built-in electric field at the InAlAs/InGaAs interface, which is correlated with the electron transfer efficiency.[16] When the ratio is larger than 2, the electron transfer efficiency is high and the corresponding device results are good.[9,16] From Fig.4, it can be seen that the photoluminescence intensities of the two peaks vary with V/III ratio. The V/III ratio affects the PL property though changing the crystal quality during the MBE growth. The intensity ratio between the two peaks is only 0.69 in sample B. In sample C with a V/III ratio of 40, the intensity of the peak is strongest and the two peak intensity ratio is 2.12. In sample D with a V/III ratio of 50, the intensity ratio between the two peaks is 2.17, but the intensity

of the peak is not larger than that of sample C. Note that when the V/III ratio is 40 in sample C, the transfer efficiency of the electron from the δ-doped InAlAs layer to the InGaAs channel is high and the built-in electric field at the $In_{0.53}Ga_{0.47}As/In_{0.52}Al_{0.58}As$ interface is strong.[17] The strong built-in electric field causes more electrons to reside in the second electron subband (e_2), so the intensity of the e_2-hh_1 transition is high and that of the e_1-hh_1 transition is low. Because the mobility of the electrons in the second electron subband (e_2) is higher than in the first electron subband (e_1) energy state,[18−20] the sample C has the highest electron mobility. From the Hall measurement, we can also find the same conclusion. Therefore sample C has the best V/III ratio.

4. Conclusions

In this paper, we report the effect of V/III ratio on the properties of MMHEMT structures grown on GaAs (001) substrates by MBE. The samples are analysed by using AFM, Hall measurement, and low temperature PL. In a range of 15–60, the optimum V/III ratio for the growth of MMHEMT structures is found to be around 40. At this ratio, the material has the following properties: a RMS roughness of only 2.02nm; a room-temperature mobility of 10610.0$cm^2/(V{\cdot}s)$; and a sheet electron density of $3.26\times10^{12}cm^{-2}$. There are tow peaks in the PL spectrum of the structure, which is corresponding to two sub-energy levels of the $In_{0.53}Ga_{0.47}$(A·s) quantum well, and their intensities vary with V/III ratio. When the V/III ratio is 40, the intensities of the peaks are strongest and the ratio between two peak intensities is large than 2. This indicates that under this V/III ratio, the built-in electric field at the $In_{0.53}Ga_{0.47}As/In_{0.52}Al_{0.58}As$ interface is strong. The majority of the electrons populate in the second electron subband (e_2) which makes the MMHEMT material have a high electron mobility.

References

[1] Chao P C 1990 *IEEE Electron Device Lett.* **11** 59
[2] Ho P, Kao M Y, Cho P C, Duh K H G, Ballingall J M, Allen S T, Tessmer A J and Smith P M 1991 *Electron. Lett.* **27** 325
[3] Behet M, Zanden K van der, Borghs G and Beheres A 1998 *Appl. Phys. Lett.* **73** 2760
[4] Dumka D C, Hoke W E, Lemonias P Cueva J G and Adesida I 1999 *Electron. Lett.* **35** 1854
[5] Bollaert S, Cordier Hoel Y V, Zaknoune M, Happy H, Lepilliet S and Cappy A 1999 *IEEE Electron Device Lett.* **20** 123
[6] Gao H L, Li D L, Zhou W Z, Shang L Y, Wang B Q, Zhu Z P and Zeng Y P 2007 *Acta Phys. Sin.* **56** 4955(in Chinese)
[7] Robin F C Farrow 1995 *Molecular Beam Epitaxy: Applications to Key Materials* (Park Ridge, NJ: Noyes) pp200–205
[8] Higuchi Y, Uemura M, Masui Y, Kitada T and Shimomura S 2003 *J. Cryst. Growth* **251** 80
[9] Stringfellow G B and Su L C 1995 *Appl. Phys. Lett.* **66** 3155
[10] Gold A 1987 *Phys. Rev.* B **35** 723
[11] Ramvall P, Carlsson N, Omling P, Samuelson L, Seifert W, Stolze M and Wang Q 1996 *Appl. Phys. Lett.* **68** 1111
[12] Lavoie C, Pinnington T, Nodwell E, T Teidje, Goldman R S and Kavanagh K L 1995 *Appl. Phys. Lett.* **67** 3744
[13] Zhang S B and Zunger A 1996 *Phys. Rev.* B. **53** 1343
[14] Hashizume T, Xue Q K, Zhou J, Ichimiya A and Sakurai T 1994 *Phys. Rev. Lett.* **73** 2208
[15] Gilperez J M, Sanchez J L, Calleja E, David J P R and Reddy M 1994 *J. Appl. Phys.* **76** 5931
[16] Cao X, Zeng Y P, Cui L J, Kong M Y and Wang B Q 2001 *J. Cryst. Growth* **227** 127
[17] Cao X, Zeng Y P, Kong M Y and Wang B Q 2001 *J. Cryst. Growth* **231** 520
[18] Fu Y and Willander M 1995 *J. Appl. Phys.* **78** 3504
[19] Zheng X, Carns T K, Wang K L and Wu B 1993 *Appl. Phys. Lett.* **62** 504
[20] Li D L and Zeng Y P 2006 *Chin. Phys.* **15** 2735